29th EPS Conference on Plasma Phys. and Contr. Fusion Montreux, 17-21 June 2002 ECA Vol. **26B**, P-5.061 (2002)

Global Gyrokinetic Study of Finite β Effects on Linear Microinstabilities

G.L. Falchetto[†] and J. Vaclavik

Centre de Recherches en Physique des Plasmas,
Association Euratom-Confédération Suisse, EPFL, 1015 Lausanne, Switzerland
[†] Present address:*DRFC, Association Euratom-CEA, CEA Cadarache,*
13108 St Paul-lez-Durance, France

1. Introduction

Electromagnetic microinstabilities in tokamak plasmas are studied by means of a linear global eigenvalue numerical code, in the framework of gyrokinetic theory. The behavior of toroidal ITG modes and electromagnetic modes in the presence of finite β, of the Shafranov shift and of trapped particle dynamics is analysed. In particular the present study provides an insight on the properties of the so-called kinetic ballooning mode [1],[2] or shear-Alfvénic Ion Temperature Gradient mode [3], AITG. The threshold for the destabilization of this mode is identified and its radial structure first disclosed, owing to the global formulation.

2.The electromagnetic gyrokinetic global model

A low frequency electromagnetic perturbation is applied to a collisionless plasma, having low - but finite - β (the parallel perturbations of the magnetic field are thus neglected). Ion dynamics is described by the gyrokinetic equation; non adiabatic electrons are taken into account, with passing particles described as drift-kinetic and trapped electrons through the bounce averaged drift-kinetic equation, as in [4]. The system is closed by the quasi-neutrality equation and the parallel component of Ampère's law. The formulation is applied to a large aspect ratio toroidal configuration, with circular shifted magnetic surfaces. The system is solved in Fourier space, taking advantage of a decomposition adapted to the toroidal geometry [5, eq.3], and can be cast into the compact form:

$$\begin{pmatrix} \mathcal{M}_{\phi\phi} & \mathcal{M}_{\phi\mathcal{A}} \\ \mathcal{M}_{\mathcal{A}\phi} & \mathcal{M}_{\mathcal{A}\mathcal{A}} \end{pmatrix} \begin{pmatrix} \hat{\phi} \\ \hat{A}_{\|} \end{pmatrix} = 0 \qquad (1)$$

where each of the submatrices is a sum over the contributions from the different particle species. The solution to the electromagnetic gyrokinetic equation is provided by solving for its propagator, which comes down to solve for the trajectories of gyrocenters. As far as one neglects the Shafranov shift, which is implemented to passing particles in a second step, the gyrocenter trajectories are the same as for the electrostatic case, thus the propagator for passing ions stays as in [4], whereas an explicit form for the propagator for passing electrons is derived making use of some approximations.

2.1 Passing Electrons. Passing electrons are considered as quasi-adiabatic, meaning that the non-adiabatic electron contribution to matrix ${\mathcal{M}_{\phi\phi}}^{el.}$ is negligible, furthermore use is made of the drift-kinetic approximation and of the frequency ordering $\omega \sim \omega_{ne} \ll \bar{\omega}_{te}$, ω_{ne} and $\bar{\omega}_{te}$ being the electron diamagnetic frequency and the average electron transit frequency. This ordering allows one to retain the diamagnetic drift only in ${\mathcal{M}_{\mathcal{A}\mathcal{A}}}^{el.}$.

The circulating electron propagator is therefore:

$$\mathcal{P} = \sum_{p=0,\pm1} J_p\left(k_\perp v_{dz}/\omega_t\right)\, J_{p'}\left(k_\perp v_{dz}/\omega_t\right)\, \frac{\exp\left[i\,(p-p')(\theta+\bar{\theta})\right]}{i\left(k_\parallel v_\parallel - p\,\omega_t - \omega\right)}\Bigg|_{p'=p-m+m'} \qquad (2)$$

Remark that since the electron transit frequency is much higher than the frequencies of the modes under study, one retains just its lower harmonics $p = 0, \pm 1$, though the poloidal coupling effect is preserved. Furthermore, consistently with the frequency ordering, the Bessel functions J_0, $J_{\pm1}$ are expanded in their small argument, $k_\perp v_{dz}/\omega_{te} \ll 1$.

2.2 The Shafranov shift. The effect of finite β on the equilibrium has been taken into account separately from that due to the sole electromagnetic perturbation. One would like to point out that no use is made of the usual "$s-\alpha$" model. For the considered equilibrium, the Shafranov shift can be derived analytically by solving the Grad-Shafranov equation perturbatively. The radial derivative of the Shafranov shift is evaluated as: $\triangle' = \frac{\mu_0}{2}\, R p'\, {q_s}^2/{B_\varphi}^2$. Hence the magnetic flux and the gyrocenter trajectories are accordingly modified, giving rise to an explicit expression for the electromagnetic gyrokinetic equation which takes into account the Shafranov shift. In practice the implementation is carried out by substituting the modified wavevectors in the propagator.

3. Numerical Results

The simulations have been performed choosing a hydrogen toroidal plasma having the following magnetic geometry: $B_0 = 1.\text{Tesla}, R = 2.m, a = 0.5m$, a polynomial safety factor profile, $q_s(s) = 1.25 + 0.67s^2 + 2.38s^3 - 0.06s^4$, which satisfies $q_s(s_0) = 2$, while the magnetic shear is $\hat{s}(s_0) = 1$, $s_0 = 0.6$. The density profile and the identical electron and ion temperature profiles have been chosen $N(s)/N_0 = \exp\left[-(a\Delta s_n/L_{n0})\tanh((s-s_0)/\Delta s_n)\right]$; $T(s)/T_0 = \exp\left[-(a\Delta s_T/L_{T0})\tanh((s-s_0)/\Delta s_T)\right]$; with $\Delta s_n = 0.35$, $L_{n0} = 0.4m$, $\Delta s_T = 0.20, L_{T0} = 0.2m, T_0 = 7.5KeV$. The density $N_0 \equiv N(s_0)$ is evaluated from the value of $\beta(s_0) = 2\mu_0 N_0(T_0^e + T_0^i)/B_0^2$. Fixing a toroidal mode number $n = 7$, scans over the parameter β have been carried out, taking into account the only circulating particle dynamics and including the Shafranov shift effect, or adding trapped electrons. Note that, once the temperature T_0 is fixed, a scan over β corresponds to a scan over density.

Results, presented in Fig. 1 show a strong stabilization of toroidal ITG modes with finite β, whereas the frequency does not change much. At approximately half the value of β for which the stabilization of the ITG mode occurs, an electromagnetic mode, AITG, is destabilized. The growth rate of this mode rises rapidly, overcoming the ITG maximal growth rate already at $\beta(s_0) \simeq 1.5\%$, whereas its frequency is initially 6 times larger than the ITG's and decreases significantly with β. The threshold for the destabilization is located at half the critical value for MHD local ballooning stability, $\beta_c^{\text{MHD}}(s_0) = 2.04\%$ as computed with KINX MHD stability code.

The effect of the Shafranov shift on the stability of electromagnetic modes is also depicted in Fig. 1. One can observe that it engenders a very strong stabilization of toroidal ITG modes (diamonds) and it is already effective at very low values of β. The threshold for the stabilization occurs at a value of $\beta \simeq 0.5\%$, corresponding to a factor 10 lower than

the value obtained considering only the electromagnetic perturbation. Concerning the AITG modes, for the parameter regime analysed here one observes a complete stabilization. To highlight this effect, results from computations performed including 5% of the Shafranov shift value are also reported in Fig. 1 (dashed line with triangles). It is evident that the growth rate of the AITG mode is halved.

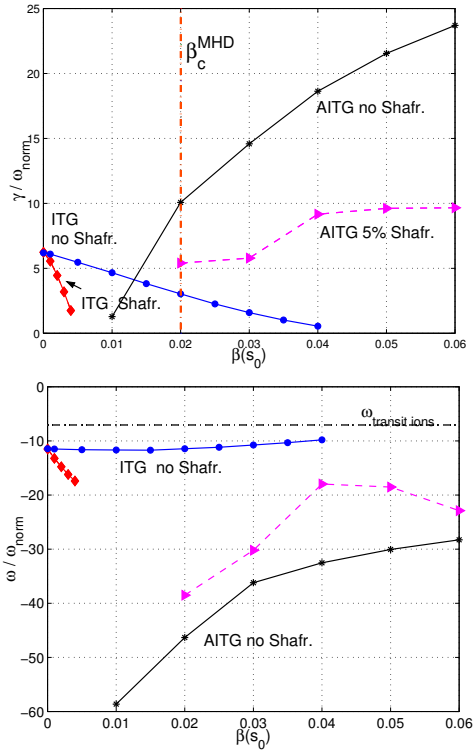

Figure 1: Normalized growth rates (top) and real frequencies (bottom) of ITG and AITG modes (full lines with circles and $*$), ITG modes with the Shafranov shift (diamonds) and AITG modes including 5% Δ' (dashed line). The local MHD ballooning limit β_c^{MHD} is also marked. $\omega_{norm} = \rho_{Li}\, v_{thi}/a^2 \simeq 3 \cdot 10^4$ Hz.

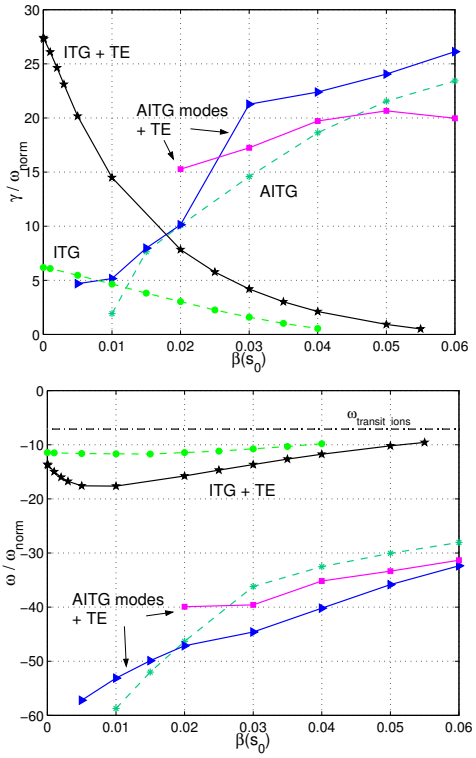

Figure 2: Normalized growth rates (top) and real frequencies (bottom) of ITG and AITG modes coupled to trapped electrons (full lines). The corresponding most unstable modes without trapped electrons are reported in dashed lines, for comparison.

Results from computations performed taking into account trapped electron dynamics have shown that the coupling to trapped electrons leads to a further destabilization of both the toroidal ITG and the AITG mode, as depicted in Fig. 2. In particular one can observe that the coupling to trapped electrons strongly enhances the ITG mode growth rate, which is then rapidly decreasing with increasing β. The complete stabilization of the coupled ITG-trapped electron mode occurs at a value of β slightly higher than for the pure ITG [5]. From Fig. 2 it is also evident that in presence of trapped electrons, a second electromagnetic mode can eventually become dominant for some values of β; the overall effect of the coupling to trapped electrons appears to be a destabilization of the AITG mode.

A typical AITG mode radial structure is shown in Fig. 3. It is evident that the mode envelope is not smooth as for toroidal ITG modes and modulations on small radial scales appear due to high radial wavenumbers produced by electron dynamics. One can also

observe that the amplitude of the poloidal components of the electrostatic potential is maximal near the corresponding rational surfaces, for which $k_{\|}(s,m) = 0$, whereas, the poloidal components of the parallel vector potential vanish there. Remark that the mode is not radially localized around the magnetic surface where the temperature gradients are maximum, but around different rational surfaces, generally much inner, depending on the value of β. The mode structure in the poloidal plane is shown in Fig. 4, for an AITG mode at $\beta = 6\%$ and for the same mode coupled to trapped electrons. One can observe that the structure reflects the behavior of the potential poloidal components and the ballooning character of the mode is more pronounced when it is coupled to trapped electrons.

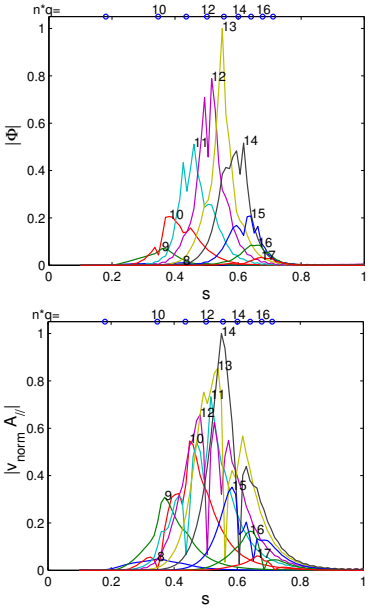

Figure 3: Poloidal mode decomposition in configuration space for the electrostatic potential(top) and parallel vector potential(bottom) of an AITG mode at $\beta = 6\%$. Mode rational surface positions are reported on the top axis.

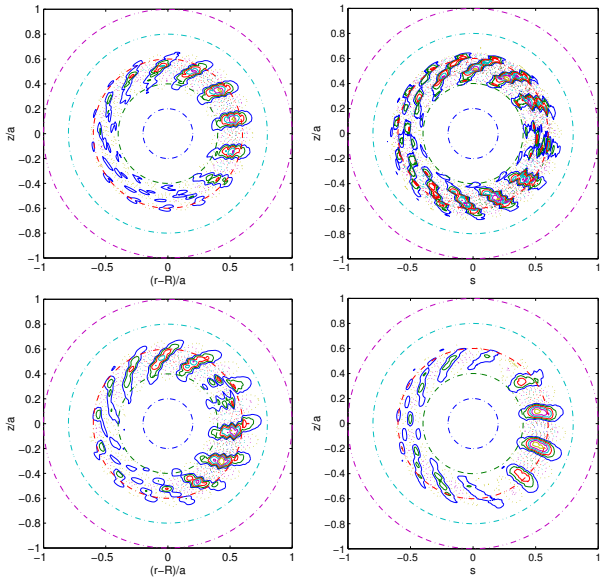

Figure 4: Contours in poloidal plane of the electrostatic potential(top) and parallel vector potential(bottom) for the AITG mode at $\beta = 6\%$ (left) and for the same mode coupled to trapped electrons (right).

Acknowledgements *One of the authors is grateful to L. Villard for stimulating discussions and acknowledges A. Martynov for the KINX computations. This work was partly supported by the Swiss National Science Foundation. The computations have been performed on the Origin 3000 of the EPFL.*

References

[1] W. Tang, J. Connor, and R. J. Hastie, Nuclear Fusion **21**, 1439 (1980).

[2] C. Z. Cheng, Physics of Fluids **25**, 1020 (1982).

[3] J. Dong, L. Chen, and F. Zonca, Nuclear Fusion **39**, 1041 (1999).

[4] S. Brunner, M. Fivaz, T. Tran, and J. Vaclavik, Physics of Plasmas **5**, 3929 (1998).

[5] G. L. Falchetto and J. Vaclavik, in *Theory of Fusion Plasmas, Proc. Int. Workshop, Varenna, August 2000* (Editrice Compositori, Società Italiana di Fisica, Bologna, 2000), p. 321.